

# GAS-JET METHOD OF METAL FILM DEPOSITION: DIRECT SIMULATION MONTE-CARLO OF He-Ag MIXTURE FLOW

N.Y. Bykov<sup>1\*</sup>, A.I. Safonov<sup>2</sup>, D.V. Leshchev<sup>1</sup>, S.V. Starinskiy<sup>2</sup>, A.V. Bulgakov<sup>2</sup>

<sup>1</sup>Peter the Great St. Petersburg Polytechnic University, Polytechnicheskaya str., 29, St.Petersburg, 195251, Russia

<sup>2</sup>Kutateladze Institute of Thermophysics SB RAS, Lavrentyev Ave., 1, Novosibirsk, 630090, Russia

\*e-mail: bykov\_nyu@spbstu.ru

**Abstract.** Nanostructured silver films were produced by the gas-jet deposition method for the temperatures of the Ag vapor source (a crucible) in the range 1200-1400K. The direct simulation Monte Carlo method was applied for modeling the silver–helium mixture flow inside the crucible with subsequent jet expansion into vacuum and detailed information on jet gasdynamics was obtained. The helium carrier gas is shown to play an important role in the deposition process by increasing both the metal atom velocity and flux onto the substrate. An optimal helium flux resulting in the maximal silver deposition rate is found. The onset of cluster formation in the Ag-He jet is determined. It is shown that for the experimental conditions silver clusters are not generated in the jet and thus the observed nanostructures are formed on the substrate surface due to diffusion and nucleation of the deposited atoms.

**Keywords:** silver films; gas-jet deposition method; direct simulation Monte Carlo; silver-helium vacuum expansion; cluster formation process.

## 1. Introduction

Thin nanostructured films of noble metals play an important role in medicine, electronics and optics due to their unique properties [1-4]. There are some different techniques of such film production including very promising gas-jet method of the metal deposition from a supersonic jet [5-8]. This method provides the evaporation of a metal inside a crucible, the mixing of a metal vapor with a carrier inert gas, the outflow of the mixture through (usually) a sound nozzle into vacuum or a low-pressure environment, the deposition of metal particles on a substrate and finally the particle assembling into a nanostructured film on the substrate surface [9-11]. The mixture expansion can be accompanied by the metal cluster formation in a flow region. Clusters that have reached the substrate can promote the formation of nanostructures on the substrate surface. Estimation of jet parameters (fluxes, velocities, temperatures of monomers and clusters) is necessary to control and optimize the gas-jet deposition technique.

The previous analysis of the flow of a metal vapor - inert gas mixture was carried out analytically and experimentally [12, 13]. Analytical estimations were based on the inviscid supersonic jet model [14] and made it possible to predict gas parameters in the far field of the jet. The gas outflow regime of interest can be near free-molecular or transient for which the characteristic Knudsen number  $Kn = \lambda_0/R > 0.01$  ( $\lambda_0$  is the mean free path determined by gas stagnation parameters inside the crucible,  $R$  is the nozzle exit radius). The use of the inviscid continuum model is questionable for mentioned above flow regimes. Within the experimental work an empirical expression for estimating the cluster formation rate inside the jet was

obtained. This expression allowed estimating the technological parameters which correspond to three possible flow patterns: (i) without clusters, (ii) with a low rate of the cluster formation and (iii) with large clusters (whose sizes exceed 100 atoms). The proposed approach did not provide detailed information on clusters size distributions, velocities and internal energies.

The modern state of computation technologies makes it possible to carry out the modeling of a motion of a metal vapor - inert gas mixture in whole flowfield including the crucible and the substrate region and obtained all necessary information of flow parameters. The most adequate method for numerical investigations of flows from free-molecular to near-continuum regimes is the direct simulation Monte Carlo (DSMC) [15]. The DSMC code may be supplemented with models of chemical reactions [16-18] including cluster formation processes [19].

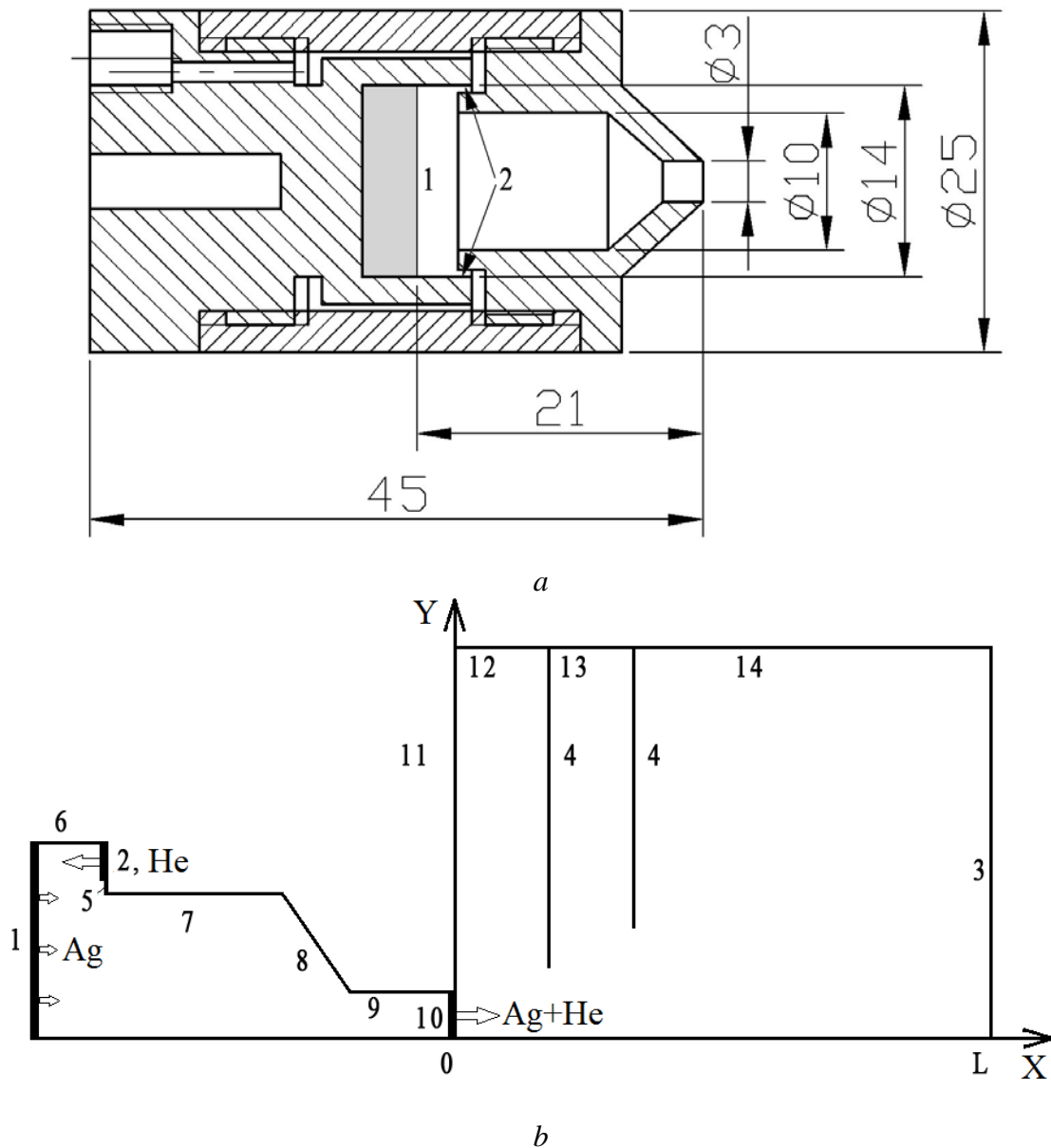


**Fig. 1.** (a) The scheme of the high-temperature source (crucible), all sizes in mm; (b) the scheme of the simulation area. 1 - the surface of the silver melt; 2 - the section of the annular helium load channel; 3 - the plane of the substrate; 4 - the shields; 5,6,7 the inner surfaces of the crucible; 8,9 - the inner surfaces of the confusor and cylindrical parts of the nozzle unit; 10 - the section of the nozzle unit; 11-14 external boundaries of the expansion zone.

The main purposes of the work are (i) to present obtained experimental data on nanostructured silver films, (ii) to investigate numerically by the DSMC method the Ag-He flow under experimental conditions, (iii) to analyze rates of the cluster formation and the possible impact of the condensation process inside the jet on the nanostructured film growth.

## 2. The nanostructured silver film deposition by the gas-jet method

The schemes of the crucible and the gas flow region for the metal film deposition technique are presented in Fig. 1. The molybdenum crucible is heated to a temperature  $T_0$ . Silver atoms are evaporated from the melt surface 1. The inert gas is loaded into the crucible with the rate  $Q$  through the annular orifice 2. The mixture of gases outflows from the nozzle exit orifice of radius  $R=1.5\text{mm}$  into the deposition chamber. The plane of the substrate 3 is located at a distance  $L$  from the nozzle exit. In order to reduce the thermal radiation heating the substrate, shields 4 are installed between the nozzle exit and substrate surface.

Thin silver films were deposited on monocrystalline silicon substrates (100). The temperature range of the crucible was  $T_0=1200\text{-}1400\text{ K}$  at a fixed flow rate of helium  $Q_{\text{He}}=36\text{ sccm}$ . The nozzle-substrate distance was varied in the range  $L=70\text{-}100\text{ mm}$ . An analysis of the morphology of films obtained under different deposition regimes was carried out by the method of Scanning Electron Microscopy (SEM, JEOL JSM-6700F microscope).

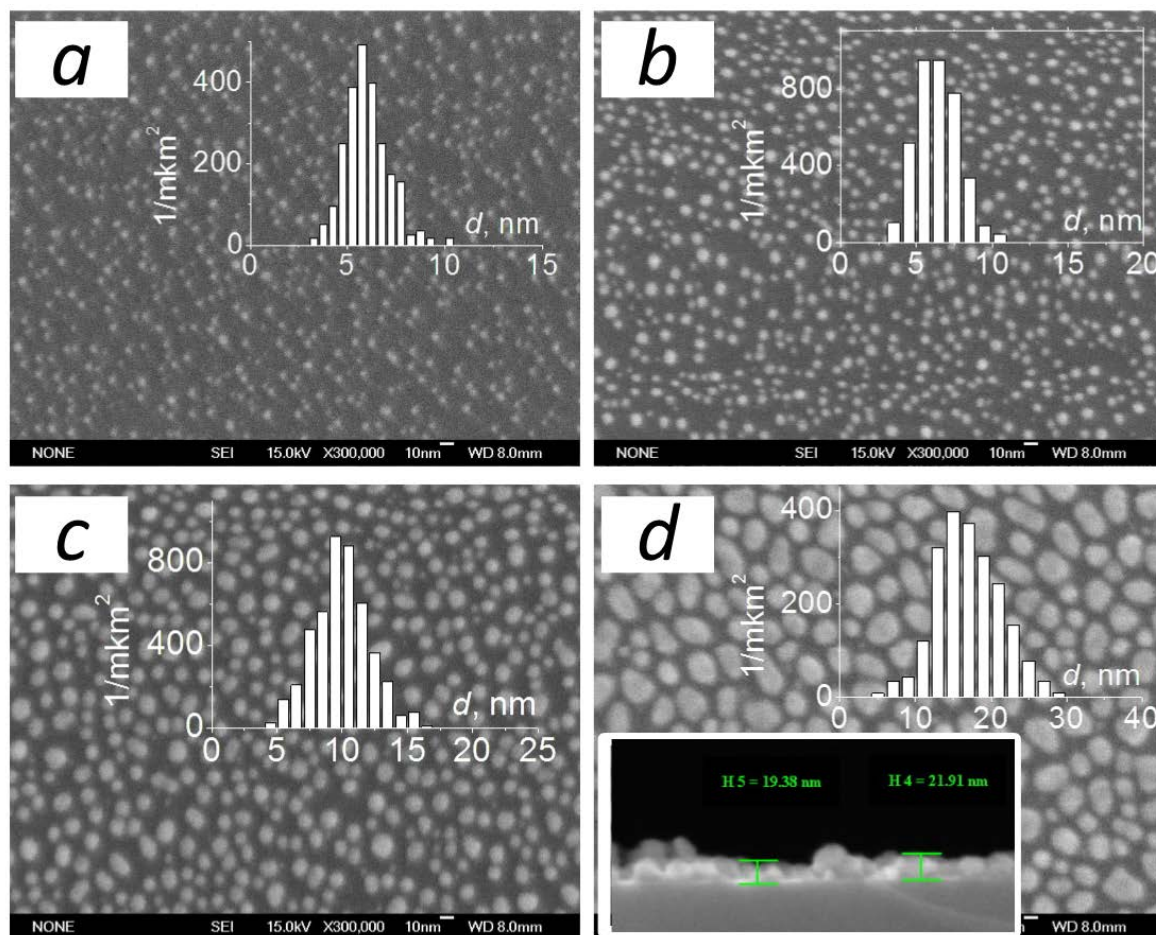


**Fig. 2.** SEM images of films deposited on the substrate, heated to 473 K. The distance to the crucible is 100 mm, the deposition time is 30 min. The source temperatures: (a) 1233 K, (b) 1276 K, (c) 1314 K, (d) 1377 K. The inserts show the histograms of the particle size distribution, and also the SEM image of the cross-section of the sample.

SEM images of silver films are shown in Fig. 2. The images were made at a fixed deposition time, but for different temperatures of the crucible. In all cases, the films are nanostructured, consisting of individual nanoparticles. The average size of nanoparticles rises with increasing of the crucible temperature from ~ 6 nm at 1233 K to ~17 nm at 1377 K. The particle size distribution is rather narrow (see histograms shown in Fig. 2). The image of the film cross-section (Fig 2, d) indicates that the nanoparticles have a shape close to spherical.

Estimations of the volume of nanostructures deposited on the surface were made and the average thickness of coatings was reconstructed. Based on these data, the fluxes of silver atoms  $F_{Ag,L}$  on the jet axis for the distance  $L=100$  mm was estimated: for  $T_0=1233$  K —  $F_{Ag,L}=4.17 \cdot 10^{16}$  m<sup>-2</sup>s<sup>-1</sup>, for  $T_0=1276$  K —  $F_{Ag,L}=5.09 \cdot 10^{16}$  m<sup>-2</sup>s<sup>-1</sup>, for  $T_0=1314$  K —  $F_{Ag,L}=1.36 \cdot 10^{17}$  m<sup>-2</sup>s<sup>-1</sup>, for  $T_0=1377$  K —  $F_{Ag,L}=2.69 \cdot 10^{17}$  m<sup>-2</sup>s<sup>-1</sup>.

The questions arise on (i) the influence of the carrier gas on the deposition process and (ii) the possibility of the cluster formation process directly in the jet volume. The deposited clusters which formed in the jet can play a role of precursors for surface nanostructures growth process. The answers can be obtained with the help of modeling by the direct simulation Monte Carlo method.

### 3. The direct simulation Monte-Carlo of He-Ag mixture flow for the temperature range $T_0=1230-1380$ K

Simulations were carried out by the DSMC method for the axisymmetrical domain (Fig. 1b). The flux of silver evaporated atoms through the surface  $l$  corresponds to the Hertz-Knudsen equation

$$F_{Ag}^+ = n_{0,Ag} \left( 8kT_0 / (\pi m_{Ag}) \right)^{1/2} / 4, \quad (1)$$

where  $n_{0,Ag}(T_0)=p_{0,Ag}(T_0)/(kT_0)$  is the equilibrium concentration of the silver vapor at a temperature  $T_0$ ,  $m_{Ag}$  is the mass of a silver atom. The saturation pressure  $p_{0,Ag}(T_0)$  is defined according data of [20].

The flux of helium inside the crucible can be defined from the known load  $Q_{He}$  with the additional assumption about the value of speed relation at the inlet section  $s = V_{He}/(2kT_0/m_{He})^{1/2}$  ( $V_{He}$  — the velocity of helium gas,  $m_{He}$  — the helium atom mass). For considering case  $s \ll 1$  and the value  $s=0.1$  was used in simulations.

Silver atoms returning back to the evaporating surface are condensed on it (are removed from simulation). Collisions of silver and helium atoms with other internal surfaces of the crucible (5, 6, 7, 8, 9) are supposed to be diffusive with full energy accommodation and temperature  $T_0$ . Helium atoms are reflected diffusively with full energy accommodation from the evaporating surface  $l$ . Atoms of helium returning back to the inlet surface 2 are reflected specularly from it. All atoms leaving computation domain through surfaces 3, 11, 12, 13, 14 are excluded from simulation processes. The surfaces of shields condense all Ag atoms and reflect (with full accommodation energy and temperature  $T_0$ ) He atoms. At the beginning of calculations ( $t = 0$ ,  $t$  is the time) there are no particles in simulation region.

The variable hard sphere (VHS) model with parameters [15]  $d_{ref,He} = 2.33$  Å,  $T_{ref,He}=273$  K,  $\omega_{He}=0.66$  ( $d_{ref,He}$ ,  $T_{ref,He}$  — reference values of collision diameter and temperature,  $\omega_{He}$  — parameter defined by viscosity dependence on temperature) was employed. The diameter of Ag atoms is supposed to be constant (the hard-sphere model (HS)) and equal to the van der Waals diameter 3.44 Å [21].

The parallel algorithm based on decomposition of the domain was employed for computer simulations.

The main parameters that determine the flow pattern under considering problem setting are the crucible (and shields) temperature  $T_0$ , the helium load rate  $Q_{He}$ , the geometric sizes and relative locations of the crucible and shields. The Knudsen numbers  $Kn_{0,Ag}=\lambda_{0,Ag}/R$  and  $Kn_{0,He}=\lambda_{0,He}/R$  ( $\lambda_{0,Ag}$  — the mean free path of Ag atoms estimated by equilibrium

concentration  $n_{0,Ag}(T_0)$ ,  $\lambda_{0,He}$  — the mean free path of He atoms estimated by average helium density inside the crucible) may be introduced for the definition of the flow rarefaction degree.

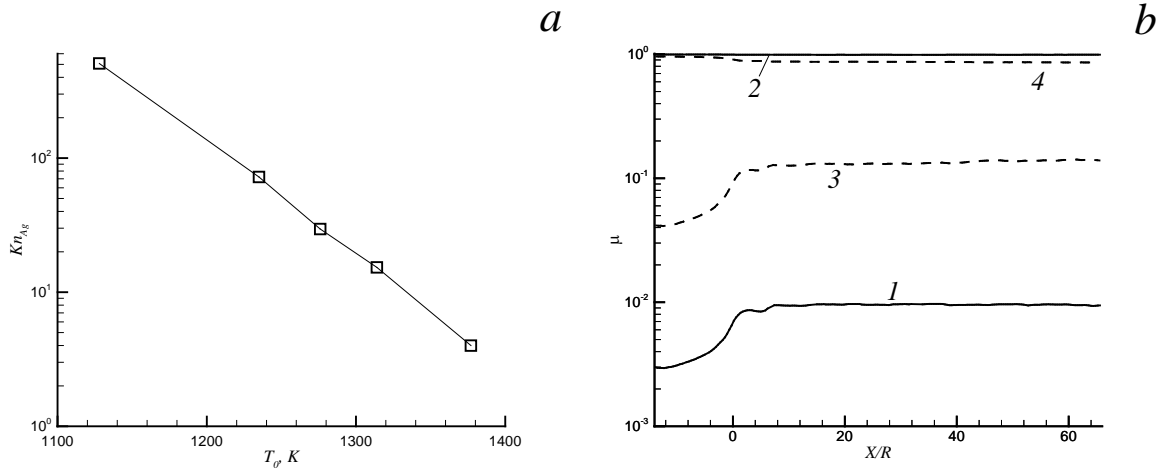


**Fig. 3.** (a) The dependence of the Knudsen number  $Kn_{Ag}$  for silver atoms on the temperature of the crucible  $T_0$ ; (b) mole fractions of silver (1, 3) and helium (2, 4) at the flow axis for the case  $Q_{He}=36$  sccm,  $T_0=1233$  K (1,2) and  $T_0=1377$  K (3,4).

The temperature dependence of Knudsen number for the Ag vapor is presented in Fig. 3a.  $Kn_{0,Ag} \gg 1$  for all considered crucible temperatures, silver atoms move without mutual collisions. The He load of 36 sccm leads to helium densities inside crucible of near  $5.6 \cdot 10^{21} \text{ m}^{-3}$  that corresponds to  $Kn_{0,He} \approx 0.6$ . The outflow of the Ag-He mixture from the crucible occurs in the transient regime. According to the data presented in Fig. 3b the Ag mole fraction in the mixture is small. The silver mole fraction increases during expansion process and “freeze” at the distance approximately  $15R$  from the crucible. For the temperature  $T_0=1377$  K at a helium flow rate  $Q_{He}=36$  sccm the mole fraction of silver atoms inside the crucible is near 4,5% and in the jet far field is about 12%.

The typical axial distributions of density, velocity and temperature of He and Ag atoms are presented in Fig. 4 for temperature  $T_0=1377$  K. Also in Fig. 4 the additional information are shown: (i) the simulation data for the case of pure Ag outflow ( $Q_{He}=0$ ), (ii) the analytical data [22] for the free-molecular outflow from a reservoir in vacuum through the orifice of radius  $R$  in the infinitively thin wall (parameters in the reservoir is supposed to be  $n_{0,Ag}$ ,  $T_0$  for the Ag jet and  $n_{0,He}$ ,  $T_0$  for the He jet), (iii) results of the simulation of inviscous continuum sound jet [14] (separately for Ag and He atoms). The location of the reservoir wall coincides with the plane of the crucible nozzle exit.

The presence of the He flux leads to increasing of Ag density within the jet and 60% silver vapor acceleration up to the value  $1.6u_0$  ( $u_0 = \{8kT_0/(\pi m_{Ag})\}^{1/2}$ ). Such value of the velocity is exceeding the value of the maximal stationary outflow of pure silver vapor into vacuum ( $\approx 1.4u_0$ ). Both Ag density and velocity are greater significantly than corresponding parameters for the case of pure Ag outflow. The presence of shields affects the He axial distributions for distances  $2 < X/R < 16$ . Temperatures of He and Ag are very close in crucible and jet far field. Parameters both He and Ag are close to free-molecular estimations rather than parameters of the continuum viscous jet. The drastic difference is observed between calculated Ag and He temperature distributions and the same distributions obtained on the basis of the inviscid jet model (Fig. 4).

To investigate the influence of the He load on the Ag nozzle flux additional calculations with values  $Q_{He}=3.6, 180, 360$  and  $1080$  sccm were carried out. The results for the crucible

temperature of 1377K are presented in Fig. 5a. With the rise of the He load the silver flux through the nozzle exit increases rapidly, achieves the maximum near the value  $Q_{He} \approx 200$  sccm and then slowly decreases. The nozzle Ag flux determines the deposition rate and as a consequence the crucible efficiency. It can be concluded that the He load in the range of 100-200 sccm for crucible temperature near 1400K is optimal for deposition technique. The reason of efficiency decreasing for high values of  $Q_{He}$  is due to the flow behavior inside the crucible where the initial helium flux is directed towards the silver evaporating surface. The low and medium values of the He load in the crucible ( $Q_{He} \approx 36$  sccm) lead to appearance of Ag density maximum near the beginning of crucible nozzle. The value of the maximum is exceeding the equilibrium density  $n_0$  (Fig. 6a). With increasing of  $Q_{He}$  the helium gas starts to compress silver atoms toward the initial evaporating surface and restrains motion of Ag toward the nozzle. The maximum of density occurs near evaporating surface and has a value about  $n_0$  (Fig. 6b).

Simulation values of the Ag atoms flux through the plane of the substrate is exceeding the same values estimated by experimental data on the film deposition (Fig. 7). The discrepancy between calculated and experimental data can be explained by the presence of a background gas (basically helium) in a deposition chamber. For the case of  $Q_{He} = 36$  sccm the pressure of the background gas in the chamber increases up to 19 Pa. The last value depends on the efficiency of a vacuum pumping system. Under low pressures of the background gas the expansion of the supersonic jet in the surrounding occurs in the regime of scattering [23] where the jet particle (in our case Ag atoms) leave the near-axial region due to the collision process. In result the Ag flux through the substrate decreases.

The background gas scattering of Ag atoms can be estimated according [24, 25]:

$$n_{Ag}(L) = n_{Ag}^0(L) \exp(-\alpha_s L), \quad (2)$$

where  $n_{Ag}^0$  — the density of silver vapor at the same distance  $L$  from the crucible without background gas scattering (vacuum conditions),  $\alpha_s = m_{He}/m_{Ag}\lambda_s$  — the attenuation coefficient,  $\lambda_s = 4/\sqrt{2n_{b,He}\pi(d_{He}+d_{Ag})^2}$  — the mean free path of Ag atoms in the background helium,  $n_{b,He}$  — the density of background gas. The factor  $m_{He}/m_{Ag}$  takes into account the low efficiency of heavy Ag atom scattering by light helium atoms. For background gas parameters  $p_{b,He} = 19$  Pa,  $T_{b,He} = 400$  K and  $L = 100$  mm we obtain  $\alpha_s = 0.45$  cm<sup>-1</sup> and  $n_{Ag}/n_{Ag}^0 = 0.011$ . This correction factor provides very good agreement between experimental and calculated data on Ag fluxes (Fig. 7,a).

To validate the background gas scattering model the silver films were deposited at the three different distances from crucible ( $L=70, 90, 100$  mm) for the temperature  $T_0=1373$  K,  $Q_{He}=36$  sccm,  $p_{b,He}=19$  Pa and the deposition time of 30 min. The film thickness was equal 8.5, 1.8 and 1 nm correspondently. Such behavior of film thickness confirms the important role of background gas scattering because the behavior of density drop differs strongly from the relationship  $L^{-2}$  that is valid for vacuum expansion. According data presented in Fig. 7b the velocity in the far field does not depend on  $L$  and the behavior of the Ag flux is governed by density drop. With taking into account the axial distribution of free jet density in vacuum and the effect of background gas scattering (eq. (2)) the silver atom flux through the substrate plane can be presented as:

$$F_{Ag}(L) = F_{e,Ag} R^2 \exp(-\alpha'_s L) / L^2, \quad (3)$$

where  $F_{e,Ag}$  — the particle flux through nozzle exit,  $\alpha'_s$  — the effective attenuation coefficient of helium scattering which should be determined by experimental data. The data on distance dependence of the film thickness were approximated by the expression (3) with the use of values  $F_{e,Ag}$  and  $\alpha'_s$  as free parameters. According data presented in Fig. 7b the considered expression describes perfectly experimental data. The obtained best fit  $\alpha'_s = 0.49$  cm<sup>-1</sup> and  $F_{e,Ag} = 1.85 \cdot 10^{22}$  m<sup>-2</sup>s<sup>-1</sup> is in good agreement with theoretical estimation for  $\alpha_s$  within relation

(2) and results of nozzle flux simulations (see Fig. 5a). Full match of data for considering case is not possible due to the approximate character of relation (3) which does not take into account variation of the silver atom velocity in the initial section of the jet. It can be concluded that the presence of background gas with densities from 1 to 20 Pa (typical for gas-jet method) leads to significant decreasing of the film deposition rate. Such decreasing can be estimated by the suggested scattering model.

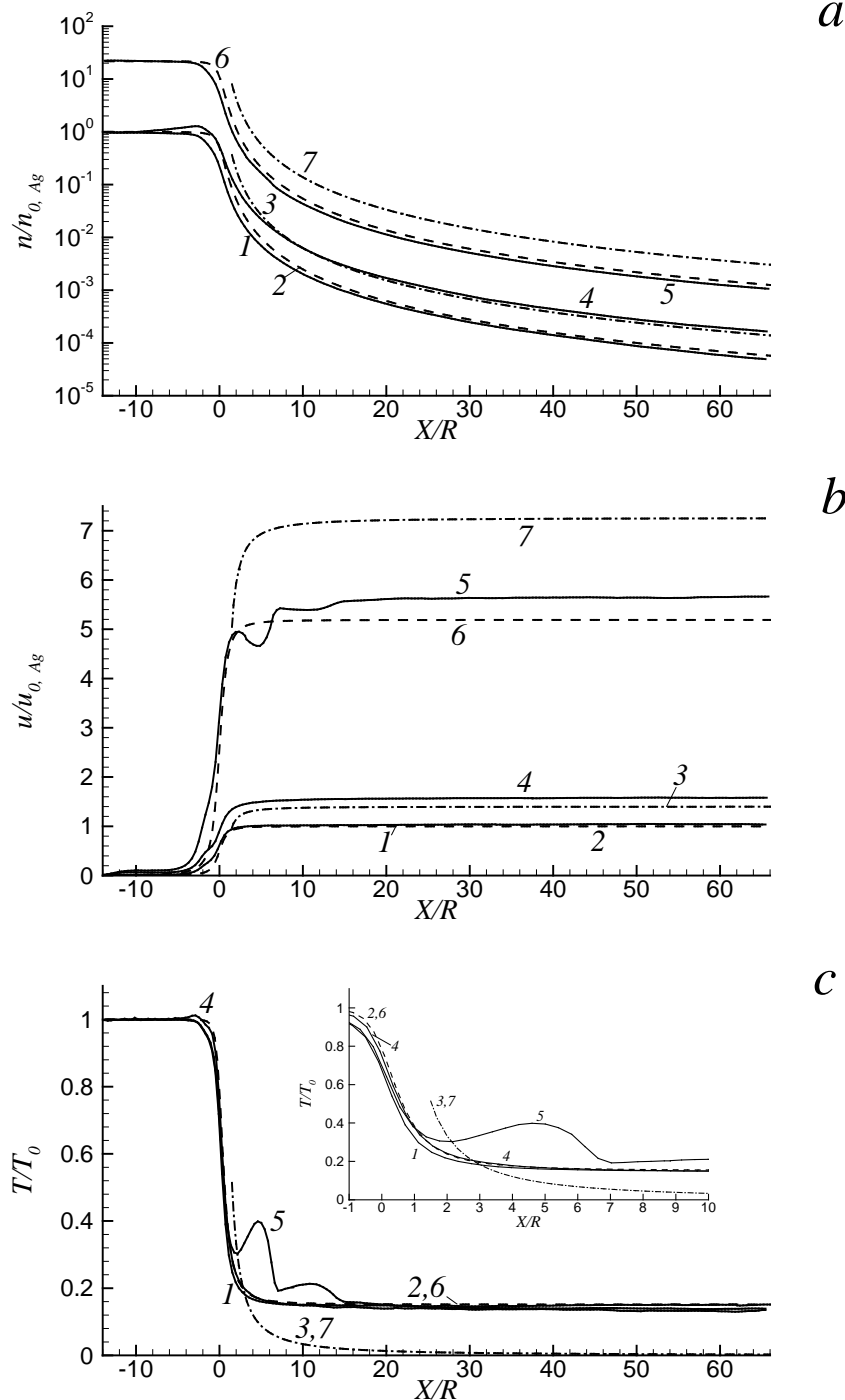


**Fig. 4.** The axial distributions of concentration (a), velocity (b), and temperature (c) for the pure silver jet (curve 1,  $Q_{He}=0$ ) and gases in the Ag-He mixture ((4) silver, (5) helium,  $Q_{He}=36$  sccm).  $T_0=1377$  K. Curves 2 and 6 are the solution [22] for the free-molecular flow of silver and helium atoms, respectively, curves 3 and 7 are the solution [14] for the inviscous jet of silver and helium atoms, respectively.

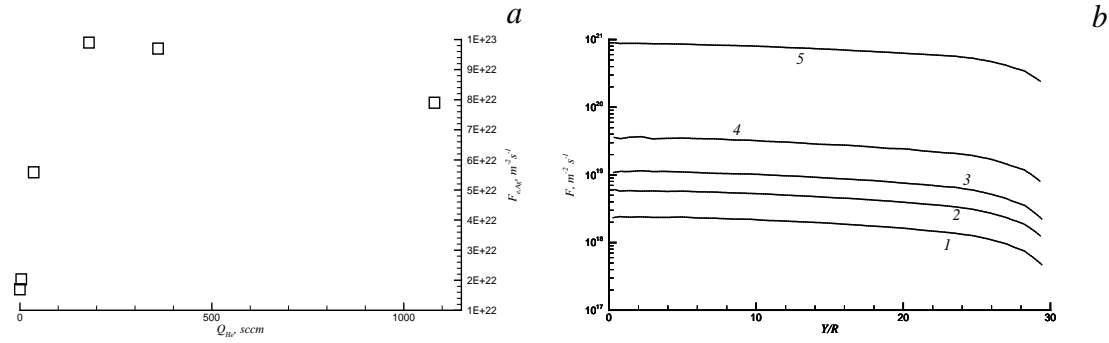


**Fig. 5.** (a) The dependence of the flux of silver atoms through the nozzle exit on the helium load for  $T_0=1377$  K; (b) the transverse distribution of the atom flux at a distance of 100 mm from the crucible (1 — Ag,  $T_0=1235$  K; 2 — Ag,  $T_0=1276$  K; 3 — Ag,  $T_0=1314$  K; 4 — Ag,  $T_0=1377$  K; 5 — He,  $T_0=1235$  K).

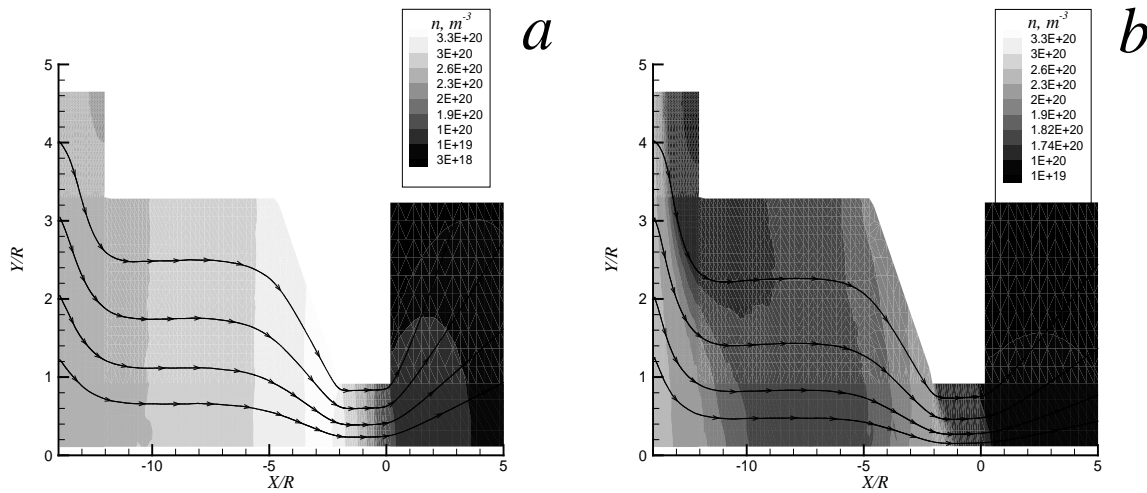


**Fig. 6.** The fields of the density and streamlines for silver atoms in the crucible for  $T_0=1377$  K. (a)  $Q_{He} = 36$  sccm, (b)  $Q_{He} = 360$  sccm.

#### 4. The direct simulation Monte-Carlo of cluster formation process in the He-Ag mixture jet

To estimate the impact of cluster formation process in the jet volume on technological parameters additional simulations were carried out. Within the DSMC method the condensation process was considered via taking into account next reactions:



Here the index 2 relates to dimers and the index  $g$  relates to clusters which consist of  $g$ -monomers. The rates of forward reactions (4), (5), (6) and reverse reactions (7), (8), (9) are denoted as  $K_{I(3),Ag}$ ,  $K_{I(3),He}$ ,  $K_{g-1}$  and  $K_{2c,Ag}$ ,  $K_{2c,He}$ ,  $K_g^-$  correspondedly. The equilibrium constant of dimerization is supposed to be  $K_C = K_{2c,Ag}/K_{I(3),Ag} = K_{2c,He}/K_{I(3),He} = AT^B \exp\{-E_a/(kT)\}$  ( $E_a$  – the activation energy,  $A$  and  $B$  – constants). The rates of forward reactions are supposed to be  $K_{I(3),Ag} = \alpha_{Ag} T^{\beta_{Ag}}$  for (4),  $K_{I(3),He} = \alpha_{He} T^{\beta_{He}}$  for (5) and  $K_{g-1} = \alpha_g T^{\beta_g}$  for (6). Within the work next values of parameters are

considered:  $A=10.86 \cdot 10^{33} \text{ m}^{-3}\text{K}$ ,  $B=-1$ ,  $E_a=1.67\text{eV}$  according [26],  $\alpha_{\text{Ag}}=0.89 \cdot 10^{-45} \text{ K}^{-0.5} \text{ m}^6 \text{ s}^{-1}$ ,  $\alpha_{\text{He}}=3 \cdot 10^{-45} \text{ K}^{-0.5} \text{ m}^6 \text{ s}^{-1}$  и  $\beta_{\text{Ag}}=\beta_{\text{He}}=0.5$  according the simplified model of triple collisions [19, 27],  $\alpha_g$  is supposed to be function only of cluster size  $\alpha_g(g_{\text{Ag}})$ ,  $\beta_g=0.5$  [19]. The probabilities of all reactions were defined for DSMC method by the total collision energy (TCE) model according [15, 19].

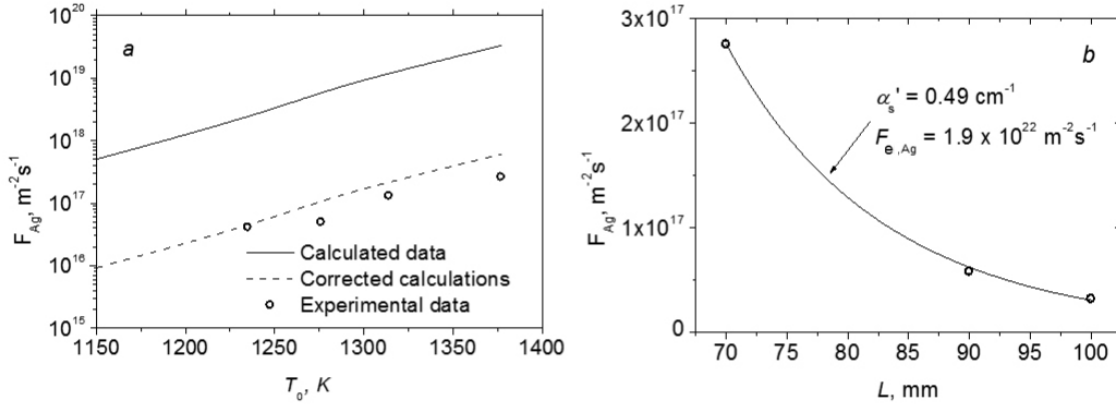


**Fig. 7.** (a) The simulation and experimental dependences of the silver atoms flux through the substrate on the crucible temperature. The dashed curve corresponds to the simulation results, corrected for the background gas scattering of Ag atoms by the equation (2); (b) the experimental dependence of the Ag flux on the substrate on the crucible distance, the curve is the approximation by equation (3).

Other parameters necessary for condensation process modeling [19] are the parameter that defines atom surface density of a cluster  $\omega_{Zh}=0.81$  [28], coordination number for liquid silver  $N_{Zh}=8.5$  [28], the radius of atom determined by density of liquid  $\rho$ :  $r_{w,\text{Ag}}=(3m/(4\pi\rho))^{1/3}=1.68 \text{ \AA}$ , the distance between atoms in the silver dimer  $r_d=1.265 \text{ \AA}$  [29], the binding energy of a silver atom on a plate surface  $\varepsilon_s=2.77 \text{ eV}$ , the dissociation energy of a silver dimer  $\varepsilon_2=1.67 \text{ eV}$  [26], the characteristic frequency of monomer vibrations inside a cluster  $\nu_0=10^{12} \text{ s}^{-1}$  [30]. The energy exchange under particle collisions was described by Larsen-Borgnakke model [15]. The probability of exchange between translation and internal modes under particle collisions was 0.1. The number of vibration degrees of freedom of a silver dimer was  $Z_{v,2}=1$ , for other clusters with size  $g$  was  $Z_{v,g}=3g-6$ .

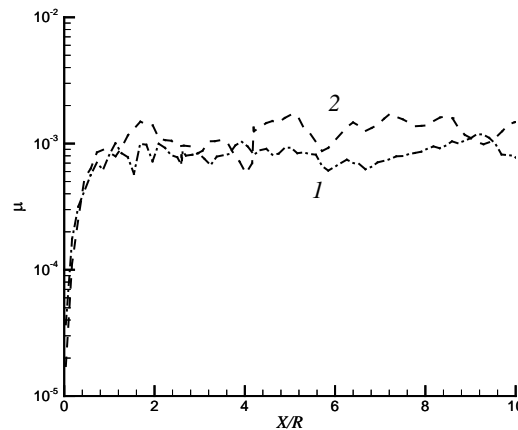


**Fig. 8.**  $\text{Ag}_2$  mole fraction in the silver jet (1) and in the Ag-He jet (2).

The DSMC modeling with taking into account condensation process were carried out for the domain limited by the nozzle exit and distance  $15 R$  from it in the  $X$  direction. The height of the computation domain was  $10 R$ . Boundary parameters at the plane of nozzle exit corresponds to parameters obtained within the computation in whole domain without taking into account the cluster formation process.

The simulation data show that there are no clusters in the jet for considered parameters of silver film deposition ( $Q_{He}=36$  sccm and  $T_0 < 1400$  K). Such conclusion is in agreement with estimations of [13]. In [13] for description of cluster formation process the parameter  $\Gamma^* = \Gamma / \Gamma_{ch}$  was employed, where  $\Gamma = n_0 d^{0.85} T_0^{-1.29}$ ,  $d = 2R$ ,  $n_0$  — the gas density inside crucible ( $\Gamma_{ch}$  depends on vapor properties). For considering cases  $\Gamma^* < 200$  and according [12, 13] there is no cluster formation process within the jet.

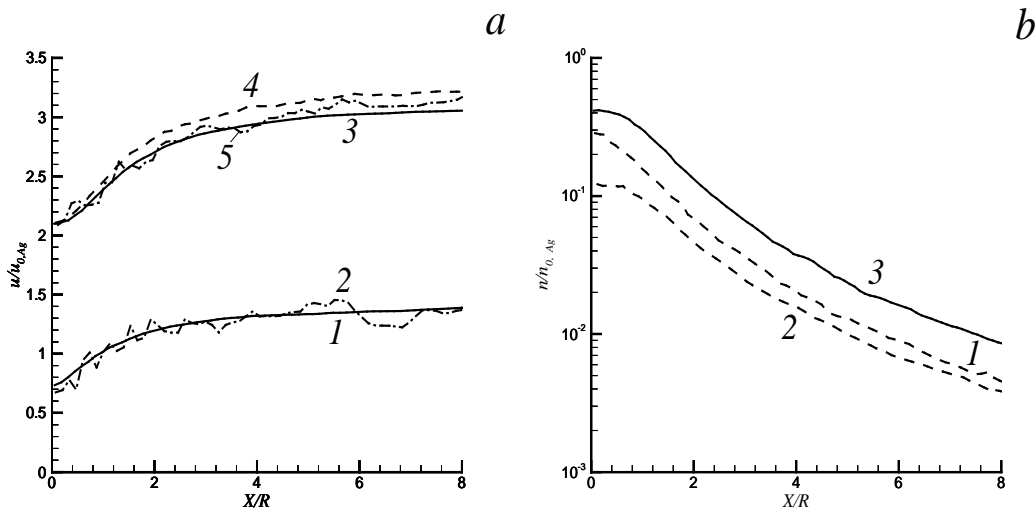


**Fig. 9.** (a) The velocity of particles in the silver jet (1 – Ag, 2 – Ag<sub>2</sub>) and in the Ag-He jet (3 – Ag, 4 – He, 5 – Ag<sub>2</sub>). (b) The dimensionless density of silver atoms in the pure silver jet (1), silver atoms in the Ag-He jet (2), helium atoms in the Ag-He jet (3).  $T_0 = 2123$  K.

To define the parameters which correspond to the cluster appearance in the jet additional simulations were carried out (i)  $T_0=1770$  K,  $Q_{He}=0$ , (ii)  $T_0=1770$  K,  $Q_{He}=1000$  sccm, (iii)  $T_0=2123$  K,  $Q_{He}=0$ , (iv)  $T_0=2123$  K,  $Q_{He}=5000$  sccm.

The mole fractions of clusters in flowfield occur very small and less than  $10^{-5}$  for the cases (i) and (ii). The main component of clusters is a dimer. The flow was rarefied for these cases, Knudsen numbers determined by parameters of gases in the crucible exit are in the order of 0.1. For higher value of the evaporation temperature  $T_0=2123$  K mole fractions of clusters in the jet are approximately  $10^{-3}$  (Fig. 8). Mole fractions of clusters are freezing at distance 1-2  $R$  from the nozzle exit which is in agreement with the data of [31]. The maximal observed within simulation cluster size is 4 atoms. The helium load of  $Q_{He}=5000$  sccm leads to acceleration of Ag atoms and clusters (Fig. 9a). The velocities of observed clusters are coincides approximately with the velocity of silver atoms. For such small flow clusterization degree there is no impact of condensation process on monomers parameters. The curves 1,3,4 in Fig. 9a and curves 1-3 in Fig. 9b coincide for the cases with and without taking into account cluster formation reactions.

## 5. Nanostructured silver film growth

Based on the set of experimental and calculated data, we can conclude that within considering experimental range of deposition parameters ( $T_0 < 1400$  K,  $Q_{He}=36$  sccm) the formation of

nanostructured film on the substrate surface occurs due to deposition of silver atoms only. The clusters in the jet is practically absent. The growth of the nanostructured film in this case occurs according to the Volmer-Weber mechanism [32]. The deposited atoms diffuse over the surface and nanoparticle nuclei are formed under collisions of such adatoms. The nonmonotonic dependence of the surface particle concentration (Fig. 2) proves this mechanism of nanostructure growth. After the stage of the surface nucleus formation process the next stage of particle size increasing begins. Then particle coagulation, the formation of “islands” of irregular form and transition to the percolation structure of the film are observed. The further rise of depositing mass leads to the formation of solid metal coating.

## 6. Conclusions

Nanostructured silver films were obtained by the gas-jet technique for the range of crucible temperatures  $T = 1200\text{-}1400\text{ K}$ . The direct simulation Monte Carlo method was applied for modeling the flow of a mixture of the silver vapor with a helium carrier gas inside the crucible with subsequent expansion of the mixture into vacuum as a free jet. The analysis of simulation and experimental data showed the following:

1) The increase of the helium flux for a fixed crucible temperature leads to non-monotonic behavior of the silver atom nozzle flux. Firstly the silver flux rises, reaches a maximal value and then slowly decreases. The helium gas accelerates the silver atoms that results in significant rise of the mass flow rate of silver vapor. As a result, the presence of the carrier gas promotes the rise of the silver flux to a remote substrate which is a positive factor for film deposition by the gas-jet method. The silver flux distribution along the substrate surface is found to be fairly uniform that is also an advantage of the considered deposition technique.

2) The presence of a background gas in the vacuum chamber leads to decrease of the silver atom flux onto the substrate and thus reduces the deposition efficiency. A simple scattering model can be used for estimation of the effect of background gas in the deposition process.

3) There are no clusters formed in the jet for the considered conditions (the crucible temperature is below 1400K and helium load is less or equal 36 sccm). The cluster formation process starts in the jet at sufficiently higher crucible temperatures and helium fluxes.

4) The flow estimations based on the inviscid continuum model are very rough and does not match the considered flow regimes. Estimations of silver vapor flow parameters for low temperatures of the crucible without carrier gas load may be done on the base of free-molecular relations. In general, DSMC (or other methods based on solving the Boltzmann equation) should be employed for adequate prediction of flow parameters.

5) The formation of the observed nanostructured silver films by the gas-jet deposition method for the considered parameter range is a result of nanocluster formation directly at the substrate surface due to diffusion and nucleation of the deposited silver atoms.

**Acknowledgements.** *This work was supported by the Russian Science Foundation (Project № 16-19-10506, experimental studies) and by the Ministry of Education and Science of the Russian Federation (Project №16.8549.2017/8.9, modeling). The computation resources were provided by the supercomputer center of Peter the Great St. Petersburg Polytechnical University.*

## References

- [1] S. Jalili, E.M. Goliaei, J. Schofield // *Int. J. of Hydrogen Energy* **42(21)** (2017) 14522.
- [2] M. Haruta // *Chem. Rec.* **3** (2003) 75.

- [3] N.R. Agarwal, F. Neri, S. Trusso, A. Lucotti, P.M. Ossi // *Appl. Surf. Sci.* **258** (2012) 9148.
- [4] S.H. Cho // *Phys. Med. Biol.* **50** (2005) 163.
- [5] I. Yamada, T. Takagi // *IEEE Trans. Electron Devices* **ED-34(5)** (1987) 1018.
- [6] P. Gatz, O.F. Hagen // *Appl. Surf. Sci.* **91** (1995) 169.
- [7] K. Wagner, P. Piseri, H.V. Tafreshi, P. Milani // *J. Phys. D: Appl. Phys.* **22** (2006) R439.
- [8] M.N. Andreev, A.K. Rebrov, A.I. Safonov, N.I. Timoshenko // *Nanotechnologies in Russia* **6(9–10)** (2011) 587.
- [9] M.J. Aziz // *Appl. Phys A* **93** (2008) 579.
- [10] C. Polop, C. Rosiepen, S. Bleikamp, R. Drese, J. Mayer, A. Dimyati, T. Michely // *New J. Phys.* **9** (2007) 1.
- [11] S.V. Starinskiy, V.S. Sulyaeva, Yu.G. Shukhov, A.G. Cherkov, N.I. Timoshenko, A.V. Bulgakov, A.I. Safonov // *J. Struct. Chem.* **58(8)** (2017) 1581.
- [12] O.F. Hagen // *Surf. Sci.* **106** (1981) 101.
- [13] O.F. Hagen // *Z. Phys. D* **20** (1991) 425.
- [14] H. Ashkenas, F.S. Sherman, In: *Rarefied Gas Dynamics*, ed. by J.H. de Leeuw (N.Y.: Academic Press, 1965), p.84.
- [15] G.A. Bird, *Molecular gas dynamics and the direct simulation of gas flows* (Clarenton Press: Oxford, 1994).
- [16] G.A. Bird // *Phys.Fluids* **23** (2011) 106101.
- [17] I.B. Sebastio, A. Alexeenko // *Physics of Fluids* **28** (2016) 107103.
- [18] S. Gimelshein, I. Wysong // *Physics of Fluids* **29** (2017) 067106.
- [19] N.Y. Bykov, Yu.E. Gorbachev // *Appl. Math. Comp.* **296** (2017) 215.
- [20] <https://www.powerstream.com/vapor-pressure.htm>
- [21] [https://www.webelements.com/silver/atom\\_sizes.html](https://www.webelements.com/silver/atom_sizes.html)
- [22] Yu.A. Koshmarov, Yu.A. Ryzhov, *Applied Dynamics of Rarefied Gas* (Mashinostroenie, Moscow, 1977). (In Russian)
- [23] A.K. Rebrov, In: *Rarefied Gas Dynamics*, ed. by O.M. Belotserkovskii (N.Y.: Springer, 1985), p.849.
- [24] A.V. Bulgakov // *SPIE Proc.* **2403** (1995) 75.
- [25] A.V. Bulgakov, M.R. Predtechensky, A.P. Mayorov // *Appl. Surf. Sci.* **96-98** (1996) 159.
- [26] B.M. Smirnov // *Phys. Usp.* **40(11)** (1997) 1117.
- [27] *Physico-chemical processes in gas dynamics. Electronic handbook in 3 volumes. Volume I: Dynamics of physico-chemical processes in gas and plasma*, ed. by G.G. Chernyi and S.A. Losev (Moscow: publishing house of Moscow University, 1995). (In Russian)
- [28] D.I. Zhukhovitskii // *J. Chem. Phys.* **101** (1994) 5076.
- [29] B.M. Smirnov, A.S. Yatsenko // *Phys. Usp.* **39** (1996) 211.
- [30] V.N. Kondratiev, E.E. Nikitin, *Kinetics and mechanism of gas-phase reactions* (Moscow: Nauka, 1974). (In Russian)
- [31] N.Y. Bykov, Yu.E. Gorbachev, V.V. Zakharov // *AIP Conf. Proc.* **1786** (2016) 050001.
- [32] J.A. Venables, G.D.T. Spliller, M. Hanbukah // *Rep. Prog. Phys.* **47(4)** (1984) 399.